Alain P. Bourgeat,Sylvie Granet, and Farid Smaï

Compositional two-phase flow in saturated–unsaturated porous media: benchmarks for phase appearance/disappearance

Abstract: The two test cases presented herein aimed at simulating the transport migration of nuclides around a nuclear waste repository and belong to the "Two-Phases Numerical Test Database" presented in [1, 2]. They were initially designed in the framework of the French research group MoMaS [3]. The starting point in designing all the test cases presented in [1] derived from some of the main challenges the traditional simulators for multiphase flow in porous media are facing when attempting to simulate gas migration in deep geological repositories for long-lived high-level nuclear waste, particularly with low-permeability argillites host rocks, as considered by most European radioactive waste management organizations and regulators (see for instance [4]). The gas migration in this type of porous media is driven by a compressible two-phase partially miscible flow, and is described by a system of nonlinear parabolic PDEs [5]. The aim of the test cases presented below and in [1] is to address some of the specific problems encountered during numerically simulating gas migration in such underground nuclear waste repositories. However, because we are interested in the difficulties inherent to physical modeling, and less in the ones coming from numerical methods, we kept a simple geometry corresponding to a quasi 1-D flow in all these test cases. The first test case is motivated by simulating the gas-phase appearance/disappearance in a two-phase flow, produced by the injection of H_2 in a homogeneous porous medium initially fully saturated with pure water. The aim of the second test case is to simulate the evolution of a compressible and partially miscible two-phase flow, starting from an out of equilibrium initial state, made up of two adjacent partially liquid saturated zones with two different uniform pressures.

Keywords: Porous Media, Multiphase Flow, Gas Migration, Nuclear Waste Repository.

Mathematics Subject Classifications 2010: 00A06, 00A69, 3502, 35K40, 35K59, 35M30, 7602, 76A99, 76S05, 76T10

Alain P. Bourgeat: Institut Camille Jordan & Université Claude Bernard Lyon 1, Villeurbanne Cedex, France, alain.bourgeat@univ-lyon1.fr
Sylvie Granet: LAMSID, UMR EDF-CNRS-CEA, Clamart, France, sylvie.granet@edf.fr
Farid Smaï: BRGM, Orléans, France, F.Smai@brgm.fr

1 Introduction

Many European countries such as Belgium, France, Germany, Sweden, and United Kingdom are presently considering the possibility of using low-permeability argillites as the host rock for future radioactive waste geological underground storage.

The main concept used in designing such geological underground storage is centered on the use of series of passive and impervious barriers made of both engineered and natural materials. The purpose of these barriers is to isolate the radionuclides and to slow down their release from the waste site into the environment. With the presence of engineered barriers in the host rock, the storage area is then a highly heterogeneous porous medium, almost fully water saturated and undergoing several water saturation–desaturation cycles during the transitory period, following the excavation, of up to 100 000 years. In addition to the low porosity and permeability of both the argillaceous host rock and the sealing materials, the strong capillary forces enhance desaturation and affect both flow pattern and the phase thermodynamic properties. The classical mathematical model for simulating the coupled transport of multiphase multicomponent flow in porous medium is based on the mass conservation for each component, and the resulting equations consist of a nonlinear and degenerated parabolic PDE system, like in [5] or [6]. Although this model can be used for a wide range of applications in geosciences, such as oil and gas reservoirs, geological CO_2 sequestration, vadose zone hydrology or NAPL remediation problems, the data and equation-of-state used in the test cases below are characteristic of water-hydrogen flow in nuclear deep geological waste disposal in low-permeability argillites. This includes, for fluids, compressibility and high contrast in densities and viscosities; as well as, for the argillaceous porous media, very low permeability (for instance between 10^{-20} and 10^{-21} m^2, for the Callovo-Oxfordian). Today's existing basic simulators for multiphase flow in porous media, in spite of their robustness could be problematic when used in such a context. Precisely, the two test cases presented here address two of the main problems in simulating com-

We wish to thank all of the teams who took part in the two test cases presented herein for their very active participation: – CERMICS, ENPC, Université Paris-Est, France and Department of Mathematics, UFSC, Brazil (Alexandre Ern and Igor Mozolevski) – IRSN and UCBL, ICJ, France (Magdalena Dymitrowska, Farid Smaï and Alain Bourgeat) – EDF, R&D, AMA, France (Ophélie Angélini, Sylvie Granet) – Friedrich-Alexander Universitat, FAU Erlangen-Nürnberg, Germany (Peter Knabner, Estelle Marchand, Torsten Muller) – ICSC Interdisciplinary Center for Scientific Computing, Universität Heidelberg, Germany (Rebecca Neumann, Olaf Ippisch, Peter Bastian) – CEA Saclay and Ecole Centrale de Nantes ECN, France (Florian Caro, Bilal Saad and Mazen Saad) – INRIA-Rocquencourt, France (Jérôme Jaffré, Ibtihel Ben Gharbia). These two test cases are part of a bigger set, the "Two-Phases Numerical Test Database" presented in [1] which has been submitted to the scientific community in January 2009. Results of the different test cases from this database were presented by several teams during the workshop "Journée Modélisation des écoulements diphasiques liquide-gaz en milieu poreux: cas tests et résultats" (see: [37]) at IHP, Paris, on September 23th, 2010.

pressible and partially miscible phases (liquid and gas) with two components (water and hydrogen) flows in such type of porous media; namely the phase appearance/disappearance and the relaxation of a nonequilibrium initial state. These two difficulties in simulating such two-phase flows were noticed in the benchmarks designed by ANDRA, The National Radioactive Waste Management Agency, (see [9–11]) and by FORGE, the Euratom 7th Framework Programme Project (see [12–14]).

In all these type of situations where physics is quite complex, there is no point in looking at the pure numerical accuracy of a code, as long as we do not have confidence in the quality of the physical modeling on which this code is based. We thought that before testing the numeric it is necessary to be sure that the simulations were simulating the real physical process. This is the reason why the aim of the two tests presented here was to focus on the model efficiency rather than on the numerical methods quality.

2 Definition and basic assumptions

In these two test cases, we consider a porous medium saturated with fluid composed of two phases, *liquid* and *gas*, and according to the application we had in mind, we consider the fluid as a mixture of two components: water (only liquid) and hydrogen (H_2, mostly gas). For the sake of simplicity, we call *hydrogen* the nonwater component and use indices w and h for the *water* and the *hydrogen* components, respectively. According to our goal, we have done some assumptions for the formulation of our model which are not essential; more general assumptions would have only complicated the present benchmark. Summarizing, we can formulate them as follows:

- Local thermal and chemical equilibrium; no reactions and only isothermal flows are considered.
- Water vaporization is neglected and the gas phase follows the ideal gas law.
- Dissolved hydrogen diffusion in the liquid phase is included and both components, water and hydrogen, diffusive fluxes, in the liquid phase are given by Fick's law.
- Water component is incompressible and the porous medium is supposed rigid.
- Both the gas and the liquid volumetric fluxes follow generalized Darcy–Muskat's law.
- Pressures are connected through a given capillary pressure law and the effects of hysteresis in the constitutive relationships are not considered.
- Adsorption of contaminants to the solid matrix is neglected.
- Concentration of the dissolved component in the water phase is low. Thus, gas dissolution can be described by Henry's law.

3 Equations

The two phases are denoted by indices, l for liquid and g for gas. Associated with each phase $\alpha \in \{l, g\}$, we have, in the porous medium, the phase pressures p_α, the phase saturations S_α, the phase mass densities ρ_α, and the phase volumetric fluxes $\mathbf{q}_\alpha$ given by the *Darcy–Muskat law*:

$$\begin{aligned} \mathbf{q}_l &= -\mathbb{K}(\mathbf{x})\lambda_l(S_l)\left(\nabla p_l - \rho_l \mathbf{g}\right), \\ \mathbf{q}_g &= -\mathbb{K}(\mathbf{x})\lambda_g(S_g)\left(\nabla p_g - \rho_g \mathbf{g}\right), \end{aligned} \tag{3.1}$$

where $\mathbb{K}(\mathbf{x})$ is the absolute permeability tensor, $\lambda_\alpha(S_\alpha)$ is the α-phase relative mobility function, and $\mathbf{g}$ is the gravitational acceleration; S_α is the effective α-phase saturation and then satisfies

$$S_l + S_g = 1\,. \tag{3.2}$$

Pressures are connected through a given *capillary pressure law*

$$p_c(S_g) = p_g - p_l\,. \tag{3.3}$$

Neglecting the water vapor and the liquid pressure influence and using the hydrogen low solubility, leads to a linearized solubility relation connecting the gas pressure, p_g and the dissolved hydrogen mass concentration in liquid, ρ_l^h: *Henry's law*,

$$\rho_l^h = C_h p_g\,, \tag{3.4}$$

where $C_h = HM^h = \rho_w^{\text{std}} M^h/(M^w K^h)$; with H being Henry's law constant, K^h being the constant specific to the mixture and M^i, $i \in \{w, h\}$, the molar mass of the i-th component. As discussed earlier, we neglect the water vaporization in the gas phase and the ideal gas law reads

$$\rho_g = C_v p_g\,, \tag{3.5}$$

with C_v being a coefficient like $C_v = M^h/(RT)$; T is the temperature and R is the ideal gas constant.

3.1 Mass conservation of each component

The water component and the gas component that are naturally in liquid state and in gas state at standard conditions are also denoted, respectively, by *solvent* and *solute*. Moreover, we assume herein, for simplicity that the mixture contains only one solvent, the *water* and one gas component, the *hydrogen*, and we write all the quantities relative to one component with the superscript $i \in \{w, h\}$.

Mass conservation for each component leads to the following differential equations:

$$\Phi \frac{\partial}{\partial t}\left(S_l \rho_l^w\right) + \operatorname{div}\left(\rho_l^w \mathbf{q}_l + \mathbf{j}_l^w\right) = \mathcal{F}^w\,, \tag{3.6}$$

$$\Phi \frac{\partial}{\partial t}\left(S_l \rho_l^h + S_g \rho_g\right) + \operatorname{div}\left(\rho_l^h \mathbf{q}_l + \rho_g \mathbf{q}_g + \mathbf{j}_l^h\right) = \mathcal{F}^h\,, \tag{3.7}$$

where Φ is the porosity; the phase flow velocities, $\mathbf{q}_l$ and $\mathbf{q}_g$, are given by the Darcy–Muskat law (3.1), and $\mathcal{F}^k$, $k \in \{w, h\}$, are the component source terms. Using the hydrogen low solubility and Fick's law, the diffusive fluxes in the liquid phase $\mathbf{j}_l^k$, $k \in \{w, h\}$, in equation (3.6) and (3.7), are given by

$$\mathbf{j}_l^h = -\Phi S_l D \nabla \rho_l^h, \quad \mathbf{j}_l^w = -\mathbf{j}_l^h, \tag{3.8}$$

where D is the hydrogen molecular diffusion coefficient in the liquid phase, possibly corrected by the tortuosity factor. Due to water incompressibility and independence of the liquid volume from the dissolved hydrogen concentration, the water component mass density in the liquid phase is constant, and in equation (3.6)

$$\rho_l^w = \rho_w^{\text{std}}, \tag{3.9}$$

with ρ_w^{std} being the standard water mass density.

4 Choice of the primary variables

An important consideration, in the modeling of fluid flow with interphase mass exchange, is the choice of the primary variables that define the thermodynamic state of the system.

If both liquid and gas phases exist, ($S_g \neq 0$), the porous medium is said to be *unsaturated*, then the transport model for the liquid–gas system can be obtained, using the traditional primary variables, saturation and one phase pressure, e.g. S_l and p_l, from equations (3.1), (3.6), and (3.7):

$$\Phi \rho_w^{\text{std}} \frac{\partial S_l}{\partial t} + \operatorname{div}\left(\rho_w^{\text{std}} \mathbf{q}_l - \mathbf{j}_l^h\right) = \mathcal{F}^w\,, \tag{3.10}$$

$$\Phi \frac{\partial}{\partial t}(S_l \rho_l^h + C_v p_g S_g) + \operatorname{div}\left(\rho_l^h \mathbf{q}_l + C_v p_g \mathbf{q}_g + \mathbf{j}_l^h\right) = \mathcal{F}^h\,, \tag{3.11}$$

$$\mathbf{q}_l = -\mathbb{K}\lambda_l(S_l)\left(\nabla p_l - (\rho_w^{\text{std}} + \rho_l^h)\mathbf{g}\right), \tag{3.12}$$

$$\mathbf{q}_g = -\mathbb{K}\lambda_g(S_g)\left(\nabla p_g - C_v p_g \mathbf{g}\right), \tag{3.13}$$

$$\mathbf{j}_l^h = -\Phi S_l D \nabla \rho_l^h\,. \tag{3.14}$$

However, in the *liquid saturated* regions, where the gas phase does not appear, $S_l = 1$, the phase saturation is no longer an unknown and the system (3.10)–(3.14) degenerates to

$$\operatorname{div}\left(\rho_w^{\mathrm{std}}\mathbf{q}_l - \mathbf{j}_l^h\right) = \mathcal{F}^w\,, \tag{3.15}$$

$$\Phi\frac{\partial \rho_l^h}{\partial t} + \operatorname{div}\left(\rho_l^h\mathbf{q}_l + \mathbf{j}_l^h\right) = \mathcal{F}^h\,, \tag{3.16}$$

$$\mathbf{q}_l = -\mathbb{K}\lambda_l(1)\left(\nabla p_l - (\rho_w^{\mathrm{std}} + \rho_l^h)\mathbf{g}\right)\,, \tag{3.17}$$

$$\mathbf{j}_l^h = -\Phi D\nabla\rho_l^h\,. \tag{3.18}$$

Consequently, when a phase appears or disappears, the set of appropriate thermodynamic variables should change, and the traditional choice for the primary unknowns, saturation and one of the phase pressure, which is used to describe unsaturated regions is no longer consistent in a fully saturated region where there is only one phase left.

There are two different approaches to this problem.

The first one, used in simulators such as [15] or [16], relies on a "primary variable substitution" algorithm in order to ensure that the Jacobian is nonsingular when phase appears and disappears. This algorithm makes use of a "persistent" variable (usually the total hydrogen concentration) in addition to the "strictly multiphasic" ones (saturation and pressure) and according to the solubility constraint, associates with each node a "component state node," on which is based the switching criterium during Newton's loop [17–20]. It is worth noticing that this method can equivalently be reformulated in the general framework of nondifferentiable but semismooth nonlinear algebraic equations, solved by means of a semismooth Newton's method implemented in terms of an active set strategy, thanks to the local character of the solubility condition [25] and [26].

The second possibility is to use a set of primary but "persistent" variables, such as pressures and component concentration, which will remain well defined when phase conditions change, so that they can be used throughout with both single and two-phase regions.

For instance, p_l and the total hydrogen concentration were used as persistent primary variables in [1]. With this choice of primary variables, the thermodynamically extended saturation and liquid pressure, appearing in the mass conservation equations, have to be recovered from the solubility conditions, coming from the thermodynamical and mechanical equilibrium assumptions. These solubility conditions (similar to "flash equations" in petroleum engineering) are formulated as a set of local inequality constraints [5] and [7]; but being local and disconnected from the space (i.e. the system is diagonal), they may be solved point-wise, by a 1-D Newton method. It is worth noting that the primary variables used in this formulation (phase pressure and total hydrogen concentration) are on one hand well adapted to problems with lit-

tle capillary effects (like in petroleum engineering) but on the other hand the ensuing Newton iterations could become cumbersome when using Van Genuchten's capillary curves. Another drawback is that these primary variables are not continuous through material interfaces in highly heterogeneous media. On the contrary the primary variables: phase pressure, p_l and dissolved hydrogen concentration, ρ_l^h, are continuous through these same interfaces.

Two of the participating teams, INRIA-Rocquencourt, France (Jérôme Jaffré, Ibtihel Ben Gharbia) and Friedrich-Alexander Universitat FAU, Erlangen-Nürnberg, Germany (Peter Knabner, Estelle Marchand, Torsten Muller), formulate the solubility conditions as complementarity constraints complementing the conservation law equations (see [24, 25] and [36]) and then use a semismooth Newton's method [21–23, 27, 28] for solving the system of nonlinear algebraic equations and constraints. A persistent variable: the total hydrogen concentration (for FAU), or the dissolved hydrogen concentration (for INRIA), is added to the strictly multiphasic ones (saturation and pressure).

The FAU's team solves the solubility conditions (considered as complementarity constraints) and the constitutive laws by a semismooth Newton algorithm inspired from [27] and the mass conservation equations by a classical damped Newton algorithm [35]. While the INRIA's team solves the two sets: the mass conservation equations and the complementarity constraints system, by a semismooth Newton method, inspired from [28].

Four other participating teams prefer to use persistent primary variables such that the recovery of the secondary variables (mainly the thermodynamically extended phase saturation) is possible through the retention curve (inverse of the capillary pressure curve). Two of them (CERMICS, ENPC, Université Paris-Est, France and Department of Mathematics, UFSC, Brazil (Alexandre Ern and Igor Mozolevski) IRSN and UCBL, ICJ, France (Magdalena Dymitrowska, Farid Smaï and Alain Bourgeat)) rely on using dissolved hydrogen concentration in the liquid, ρ_l^h, and liquid pressure, p_l as the two primary variables. Assuming that the effects of the capillary forces are not negligible, it is then possible by means of the retention curve to define the thermodynamically extended phase saturation as a function of the dissolved hydrogen concentration in the liquid, ρ_l^h, and the liquid pressure p_l (see [6, 7] and [8]). With this, the conservation laws and constitutive equations are then leading to a new system of equations able to describe both liquid saturated and unsaturated flow; see [6, 7] and [8].

The two other teams (EDF, R&D, AMA, France (Ophélie Angélini, Sylvie Granet) ICSC, Universität Heidelberg, Germany (Rebecca Neumann, Olaf Ippisch, Peter Bastian)), in a very same spirit, use as persistent primary variables two of the three pressures (p_l, p_g, or p_c) and recover the thermodynamically extended phase saturation from the retention curve; see: [29] and [30].

5 Presentation of the two test cases

We emphasize that the scope of these two following tests is oriented to the mathematical model efficiency and robustness rather than to the numerical performance issues. Mainly, the main goal of these numerical experiments is to assess flow situations involving phase appearance/disappearance or phase disequilibrium. It is clear that, in this context, the porous domain geometry does not really matter and we have considered for porous domain a porous rock core sample represented by a simple quasi-1D, porous domain (Figure 3.1), and we also neglected the gravity effects.

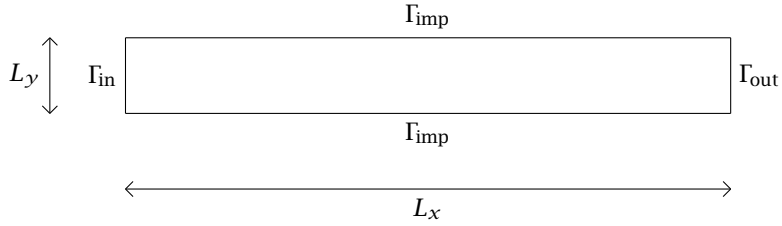

Figure 3.1: The porous medium domain Ω with its boundaries.

5.1 First test case: gas phase appearing/disappearing by gas injection in a water-saturated rock core sample

As seen earlier, it is not an easy task to simulate multiphase flow when there are both fully liquid saturated and unsaturated two-phases regions. The aim of this first test case is to study only the phase appearance/disappearance phenomenon, without mixing with any other phenomenon. This first test is devoted to describing gas phase appearance produced by injecting pure hydrogen in a 2-D homogeneous porous domain Ω (Figure 3.1), which was initially 100 % saturated by pure water. The porous domain is a rectangle of size $L_x \times L_y$ with three types of boundaries: Γ_{in}, being the inflow boundary ; Γ_{out}, the outflow boundary and Γ_{imp}, the impervious boundary (Figure 3.1).

5.1.1 Boundary and initial conditions

There is no source inside the domain:

$$\mathcal{F}^w = \mathcal{F}^h = 0\,.$$

Denoting $\phi^w \equiv \rho_l^w \mathbf{q}_l + \mathbf{j}_l^w$ and $\phi^h \equiv \rho_l^h \mathbf{q}_l + \rho_g \mathbf{q}_g + \mathbf{j}_l^h$ the total fluxes of water and hydrogen components and ν the outward normal, the boundary conditions are

- no flux on Γ_{imp},

$$\phi^w \cdot \nu = 0 \quad \text{and} \quad \phi^h \cdot \nu = 0\,;$$

- injection of hydrogen on Γ_{in},

$$\phi^w \cdot \nu = 0 \quad \text{and} \quad \phi^h \cdot \nu = \begin{cases} Q^h & \text{if } 0 \le t \le T_{\text{inj}} \\ 0 & \text{else}; \end{cases}$$

- pure liquid water with a fixed pressure, p_l, on Γ_{out},

$$p_l = p_{l,\text{out}} \quad \text{and} \quad \rho^h_{\text{tot}} = 0\,.$$

Initial conditions are uniform on all the domain and correspond to a stationary state, with no hydrogen injection :

$$p_l = p_{l,\text{out}} \quad \text{and} \quad \rho^h_{\text{tot}} = 0\,.$$

5.1.2 Physical data

The porous domain Ω is isotropic and homogeneous, the absolute permeability tensor reduces then to a scalar $\mathbb{K} = k\mathbb{I}$.

As usual in hydrogeology, the van Genuchten–Mualem model is used for defining the capillary pressure law and the relative permeability functions, i.e.

$$p_{\text{c}} = P_r \left(S_{le}^{-1/m} - 1\right)^{1/n}, \quad kr_l = \sqrt{S_{le}} \left(1 - (1 - S_{le}^{1/m})^m\right)^2$$
$$\text{and} \quad kr_g = \sqrt{1 - S_{le}} \left(1 - S_{le}^{1/m}\right)^{2m},$$
$$\text{with} \quad S_{le} = \frac{S_l - S_{lr}}{1 - S_{lr} - S_{gr}} \quad \text{and} \quad m = 1 - \frac{1}{n};$$

with parameters P_r, n, S_{lr}, and S_{gr} depending on the porous media.

The α-phase relative mobilities are then given by the relative permeability kr_α and the phase viscosity μ_α through $\lambda_\alpha = kr_\alpha/\mu_\alpha$.

The temperature is assumed to be constant $T = 303\,\text{K}$ and the corresponding porous medium parameters and fluid characteristics are shown in Table 3.1.

Parameters defining geometry, boundary and initial conditions, together with the total simulation time, T_{simul}, are presented in Table 3.2.

Table 3.1: First test case: Porous medium parameters and fluid characteristics.

Porous medium			Fluid characteristics		
Parameter	**Value**		**Parameter**	**Value**	
k	5×10^{-20}	m^2	D	3×10^{-9}	m^2/s
Φ	0.15	$(-)$	μ_l	1×10^{-3}	Pa s
P_r	2×10^6	Pa	μ_g	9×10^{-6}	Pa s
n	1.49	$(-)$	H	7.65×10^{-6}	$\text{mol}/\text{Pa}/\text{m}^3$
S_{lr}	0.4	$(-)$	M_l	10^{-2}	kg/mol
S_{gr}	0	$(-)$	M_g	2×10^{-3}	kg/mol
			ρ_l^{std}	10^3	kg/m^3

Table 3.2: First test case: Domain size; boundary and initial conditions; total simulation time.

Parameter	Value	
L_x	200	m
L_y	20	m
Q^h	5.57×10^{-6}	kg/m^2/year
$p_{l,\text{out}}$	10^6	Pa
T_{inj}	5×10^5	years
T_{simul}	10^6	years

5.1.3 Results

Six teams participated in this test case: CERMICS-UFSC, EDF, FAU, INRIA, ICSC, and IRSN-UCBL. Details concerning spatial and time discretization are given in Tables 3.3 and 3.4.

Figures 3.2, 3.3, and 3.4 give, respectively, the liquid pressure, gas pressure, and saturation levels and their time evolutions at the domain left boundary. At first glance there are some differences between different team's results concerning the "gas pres-

Table 3.3: First test case: Discretization's parameters.

Teams	Software	Spatial scheme	Mesh
CERMICS-UFSC	MATLAB	Discontinuous Galerkin	200 q.
EDF	Code_Aster [32]	Finite elements (Q1 Lagrange)	200 q.
INRIA	In-house code	Finite volume (upstream)	200 q.
IRSN-UCBL	In-house code	Finite elements (Q1 Lagrange)	200 q.
FAU	M++	Mixed hybrid FE	4480 tr.
ICSC	Dune [31]	Finite volume (upstream weighting)	400×20 q.

Table 3.4: First test case: Time discretization.

Teams	Time discretization	Time step size (years) Time step management
CERMICS-UFSC	Implicit Euler	125 to 5000 (1400 manually controlled time steps)
EDF	Implicit Euler	0.1 to 15 000 (952 manually controlled time steps)
INRIA	Implicit Euler	8000 to 50 000 (200 manually controlled time steps)
IRSN-UCBL	Implicit Euler	100 to 15 000 (183 manually controlled time steps)
FAU	Implicit for the diffusion and explicit for the convection	200 (5000 manually controlled time steps)
ICSC	Implicit Euler	0.001 to 1000 (1004 time steps; the time step is doubled after each successful step)

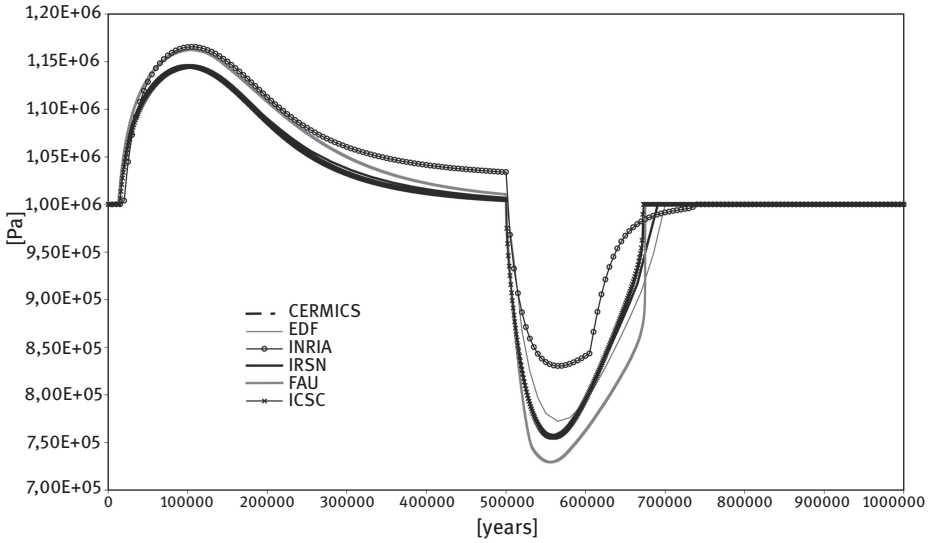

Figure 3.2: Test-case 1: Liquid pressure evolution on the left boundary of the domain.

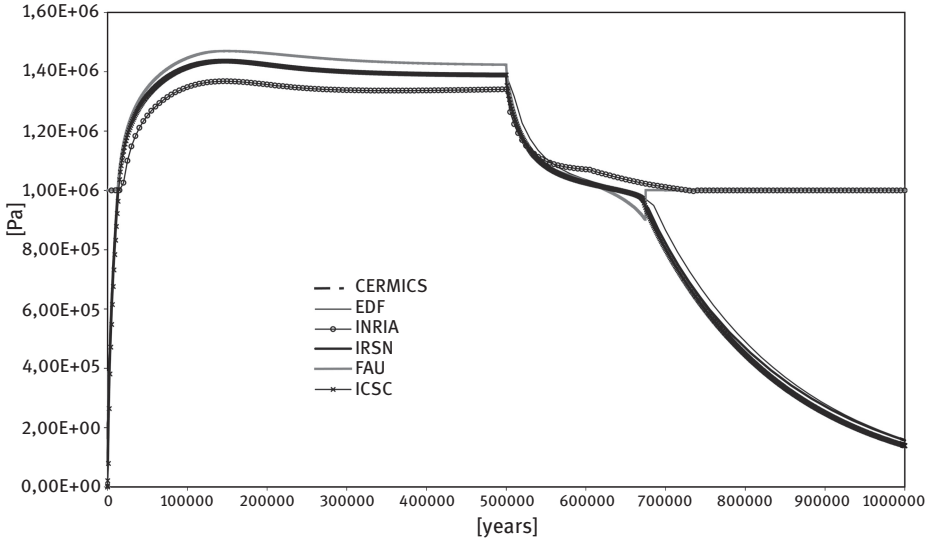

Figure 3.3: Test-case 1: Gas pressure evolution on the left boundary of the domain.

sure" curve once the porous medium is saturated. But this is due to the fact that these curves have different meanings after the gaseous phase has disappeared. Namely, in monophasic regions, where there is no more "observed" gas phase, the "represented" gas phase pressures are, for both INRIA and FAU, the liquid phase pressure, while for

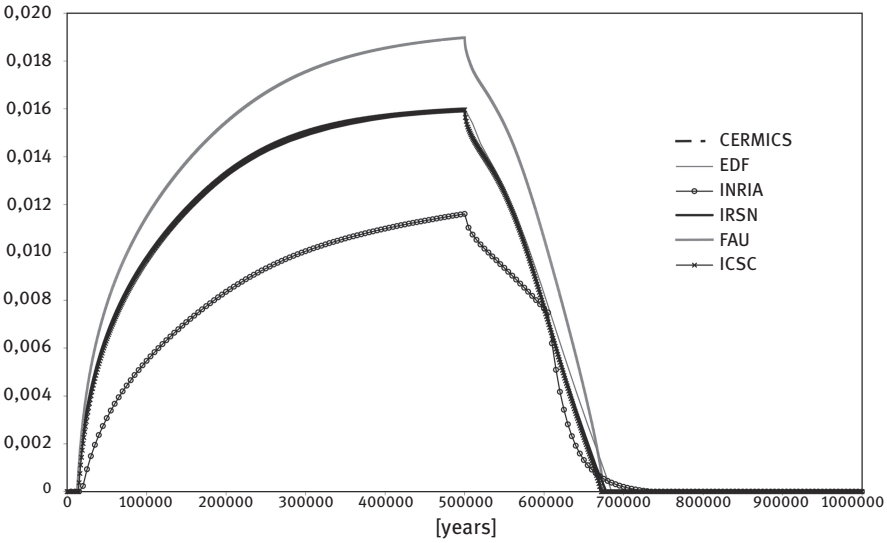

Figure 3.4: Test-case 1: Gas saturation evolution on the left boundary of the domain.

the other teams the variable named p_g represents a "thermodynamically" extended gas phase pressure (see Section 4).

Though similar phenomena and tendencies are shown by all teams:

- at the beginning ($t < 15\,000$ years), the entire hydrogen is dissolved in water and transported by diffusion; the liquid pressure remains almost constant.
  After the maximum of solubility is reached, a gaseous phase appears and both liquid and gas pressure increase up to $t \simeq 100\,000$ years.
- Between 100 000 and 500 000 years, hydrogen is still injected and consequently the gas saturation keeps growing, while both the gas and liquid pressures are decreasing.
  When the gaseous phase total volume has reached its maximum value, the liquid flux (oriented from the left to the right) slows down; the liquid pressure tends to the pressure imposed on the right boundary [29].
- After 500 000 years, when injection stops, the saturation decreases, water comes back from right to left to fill in the empty space and the liquid pressure quickly decreases on the left. Then, as the gas pressure keeps decreasing, the liquid pressure grows once more in order to reach its initial value. The gaseous phase disappears after approximately 700 000 years, i.e. about 200 000 years after the injection has ceased.

From a qualitative point of view, all the results are consistent but some differences appear in the quantitative values. Specially, some differences are observed in the results given by INRIA and FAU, for the maxima of saturation (and consequently for the liquid pressure minima), which have respectively lower and higher values than

all the other teams. Considering that the other four teams, with different schemes (discontinuous Galerkin, FE, FV), give the same results, we may assume that the spatial scheme choice is not the cause of this difference. The use of very large time step sizes by INRIA is a very likely cause of this difference. But, for FAU, further investigations have shown that these differences cannot be explained neither by the stopping criteria for the solvers nor by the Van Genuchten regularization used; clearly more investigations are required to be understood.

5.2 Second test case: evolution from an initial out of equilibrium state to a stabilized stationary one, in a sealed porous core sample

This last numerical test intends to be a simplified representation of what happens when a nonsaturated porous block is placed within a water-saturated porous structure. The challenge is then how the mechanical balance will be restored in such a porous domain, which was initially out of equilibrium, i.e. with a jump in the initial phase pressures. This may happen typically, when the engineered barriers are installed around the waste packages. The initial state is said to be out of equilibrium, because if this initial state was in equilibrium, in the two subdomains Ω_1 and Ω_2, the local mechanical balance would have made the pressures, of both the liquid and the gas phase, continuous in the entire domain Ω.

For simplicity, we consider for the porous medium domain Ω, a homogeneous and sealed core sample of concrete. It is represented by a rectangle Ω of size $L_x \times L_y$ with Γ as the boundary. All the porous medium characteristics are the same in the two subdomains Ω_1 and Ω_2, of respective length L_1 and $(L_x - L_1)$ as shown in Figure 3.5. The system is then expected to evolve from this initial out of equilibrium state toward a stationary state.

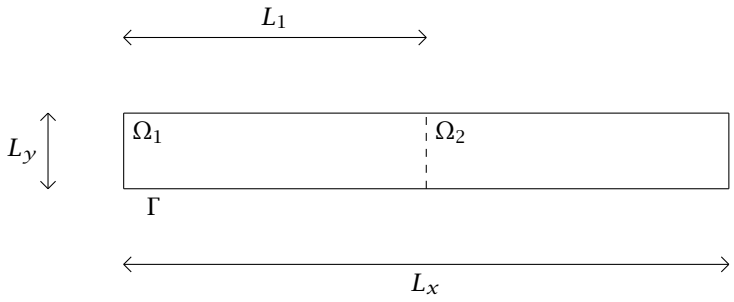

Figure 3.5: Porous domain Ω, with its two subdomains: Ω_1 and Ω_2

5.2.1 Boundary and initial conditions

There is no source inside the domain:

$$\mathcal{F}^w = \mathcal{F}^h = 0\,.$$

No-flux boundary conditions (sealed boundaries) are defined everywhere on Γ, the boundary of Ω:

$$\phi^w \cdot \nu = 0 \quad \text{et} \quad \phi^h \cdot \nu = 0\,.$$

Initial conditions are uniformly constant on each subdomain Ω_1 and Ω_2:

$$\begin{aligned} p_l &= p_{l,1} && \text{and} \quad p_g = p_{g,1} && \text{on } \Omega_1\,,\\ p_l &= p_{l,2} = p_{l,1} && \text{and} \quad p_g = p_{g,2} \neq p_{g,1} && \text{on } \Omega_2\,. \end{aligned}$$

5.2.2 Physical data

The porous medium parameters P_r, n, S_{lr} and S_{gr} are defined like in the first test case; the temperature is supposed constant, $T = 303\,\mathrm{K}$; and the fluid characteristics are shown in Table 3.5.

Parameters defining the geometry, the boundary and initial conditions, together with the total simulation time, T_{simul}, are presented in Table 3.6.

Table 3.5: Test-case 2: Porous medium parameters and fluid characteristics.

Porous medium			Fluid characteristics		
Parameter	**Value**		**Parameter**	**Value**	
k	10^{-16}	m^2	D	3×10^{-9}	m^2/s
Φ	0.3	$(-)$	μ_l	1×10^{-3}	Pa s
P_r	2×10^6	Pa	μ_g	9×10^{-6}	Pa s
n	1.54	$(-)$	H	7.65×10^{-6}	$\mathrm{mol/Pa/m}^3$
S_{lr}	0.01	$(-)$	M_l	10^{-2}	kg/mol
S_{gr}	0	$(-)$	M_g	2×10^{-3}	kg/mol
			ρ_l^{std}	10^3	$\mathrm{kg/m}^3$

Table 3.6: Test-case 2: Domain size; boundary and initial conditions; total simulation time.

Parameter	**Value**	
L_x	1	m
L_y	0.1	m
L_1	0.5	m
$p_{l,1}$	10^6	Pa
$p_{g,1}$	1.5×10^6	Pa
$S_{l,1}^{t=0}$	96.2	%
$p_{l,2}$	10^6	Pa
$p_{g,2}$	2.5×10^6	Pa
$S_{l,2}^{t=0}$	84.2	%

5.2.3 Results

Eight teams have participated in this exercise: CEA, CEA-ECN, CERMICS-UFSC, EDF, FAU, ICSC, IRSN2, and IRSN-UCBL. In this last test case, the two phases are always present; the porous medium stays, everywhere and always, liquid unsaturated. It was then possible for the CEA team to use the traditional Pressure-saturation model (with an additional residual saturation) and for the IRSN2 team to use an immiscible formulation. Taking advantage of the liquid unsaturated situation, the CEA-ECN team in a first step solves the intraphase transfer (convection/diffusion) working with liquid pressure, gas pressure and dissolved hydrogen concentration as primary variables [33] and in the second step solves the interphase transfer, using the solubility relation. The five other teams have used the same formulation as in the previous test case. The details concerning the teams spatial and time discretization are given in Tables 3.7 and 3.8.

Table 3.7: Test-case 2: Discretization parameters.

Teams	Software	Spatial scheme	Mesh
CEA	MPCube	FV Diamants	200 tr.
CEA-ECN	Scilab 1D	1-D Finite differences	200 elts.
EDF	Code_Aster [32]	Finite elements (Q1 Lagrange el.)	100 q.
FAU	M++	Mixed hybrid FE	4480 tr.
ICSC	Dune [31]	Finite volume (upstream)	100 q.
IRSN-UCBL	In-house code	Finite elements (P1 Lagrange)	500 q.
IRSN2	Migastra	FV (convection) + EF (diffusion)	200 tr.
CERMICS-UFSC	MATLAB	1-D Disc. Galerkin	521 elts.

Table 3.8: Test-case 2: Time discretization.

Teams	Time discretization	Time step size (s) Time step management
CEA	Implicit Euler	0.17 to 833 (the time step is multiplied by 1.1 after each successful step)
CEA-ECN	Implicit Euler	0.17 to 833 (the time step is multiplied by 1.2 after any successful step)
EDF	Implicit Euler	2 to 15 000 (136 manually controlled time steps)
FAU	Implicit for the diffusion and explicit for the convection	1 to 1000 (nonautomatic time steps)
ICSC	Implicit Euler	1 to 1000 (the time step is doubled after any successful step)
IRSN-UCBL	Implicit Euler	0.1 to 4000 (nonautomatic time steps)
IRSN2	Implicit Euler	1 to 16 (nonautomatic time steps)
CERMICS-UFSC	Implicit Euler	0.31 to 15 625 (288 manually controlled time steps

Figures 3.6–3.10 and Figures 3.11–3.15 give, respectively, the gas and liquid pressure levels, at $t = 10\,\text{s}$, $t = 1000\,\text{s}$, $t = 5000\,\text{s}$, $t = 50\,000\,\text{s}$, $t = 500\,000\,\text{s}$ and $t = 1\,000\,000\,\text{s}$. Figures 3.16–3.20 give saturations profiles, respectively, for $t = 10\,\text{s}$, $t = 1000\,\text{s}$, $t = 5000\,\text{s}$, $t = 50\,000\,\text{s}$, $t = 500\,000\,\text{s}$ and $t = 1\,000\,000\,\text{s}$.

All the results obtained by different teams and presented here are close and show similar trends.

As the liquid pressure "shock" in Figure 3.11 says:

- for the short times ($t = 10\,\text{s}$) the gas phase flows from right to left, due to higher gas pressure in the unsaturated part of the porous domain;
- the liquid phase is then compressed by the gas at the left part of the interface;
- and on the other domain side, the water has more space and the pressure decreases.

  This shock propagates progressively until reaching pressure equilibrium, and the global system gradually tends to equilibrium.

As for the first test case, there are some little differences between the teams results. For instance, at the simulation end ($t = 1\,000\,000\,\text{s}$, Figure 3.15), the equilibrium state is not reached yet by IRSN2. One possible reason is the use of very small timesteps (16 s versus 800 s or more, for the other teams).

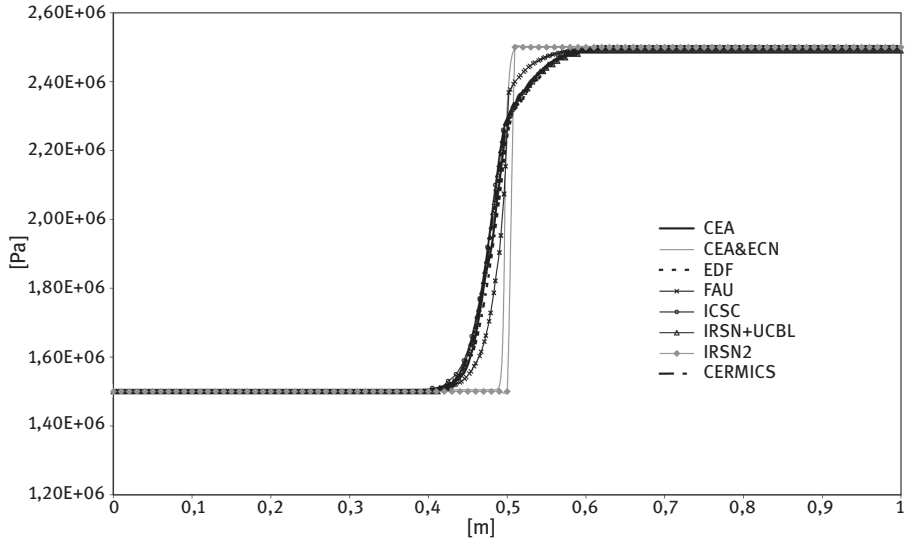

Figure 3.6: Test-case 2: Gas pressure at $t = 10\,\text{s}$.

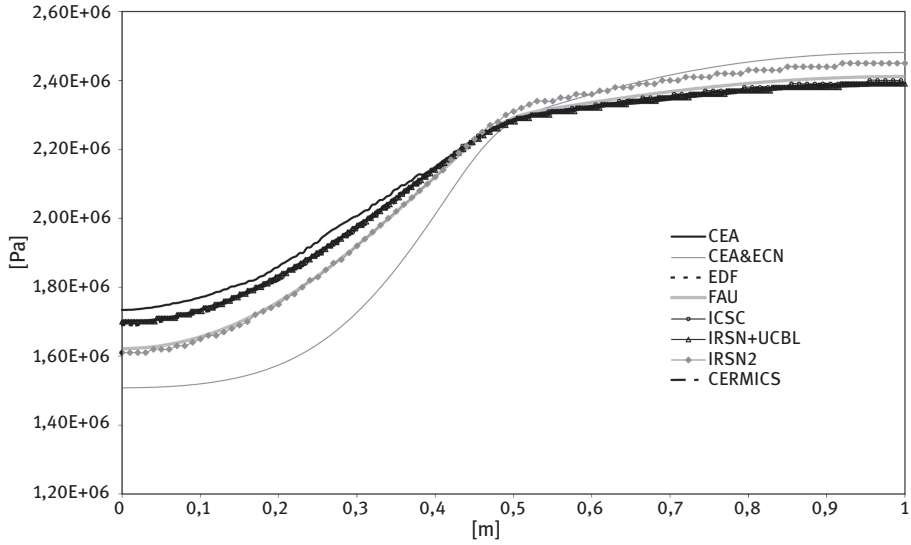

Figure 3.7: Test-case 2: Gas pressure at $t = 1000$ s.

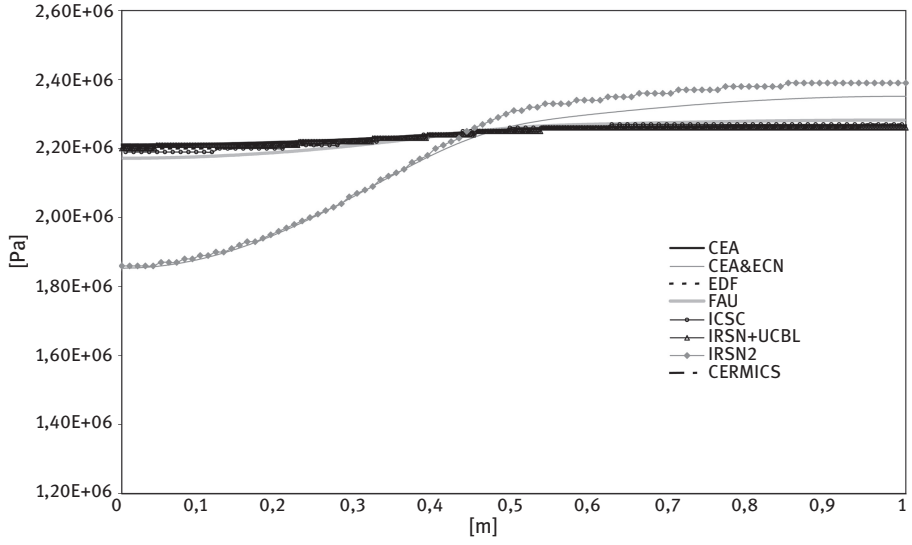

Figure 3.8: Test-case 2: Gas pressure at $t = 5000$ s.

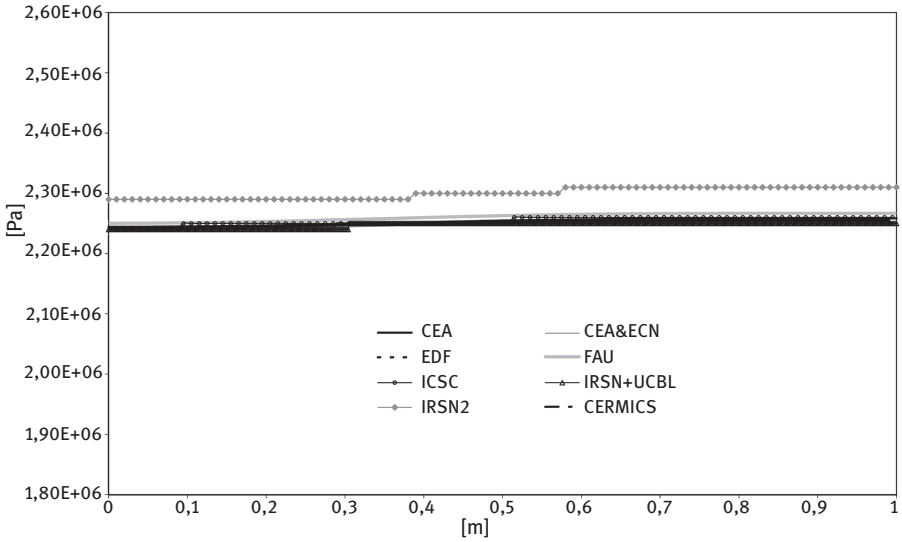

Figure 3.9: Test-case 2: Gas pressure at $t = 50\,000$ s.

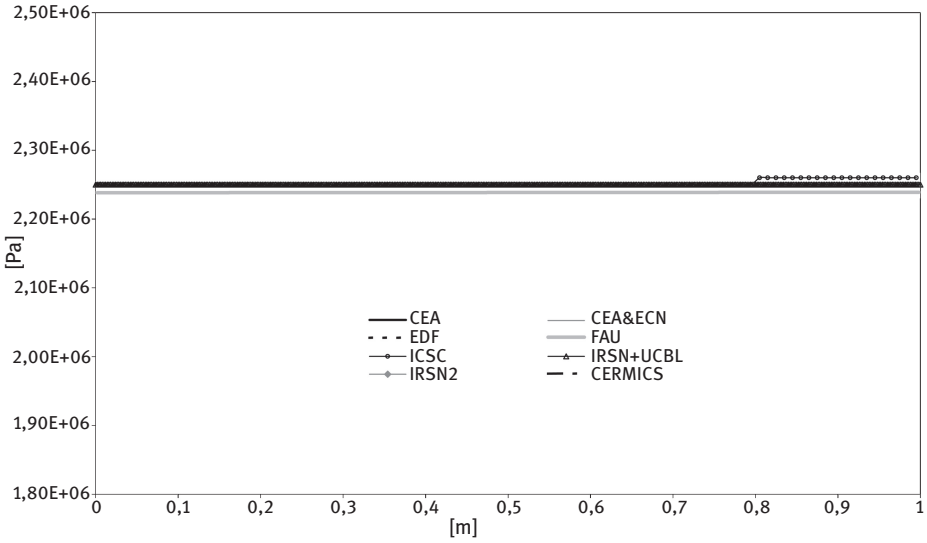

Figure 3.10: Test-case 2: Gas pressure at $t = 1\,000\,000$ s.

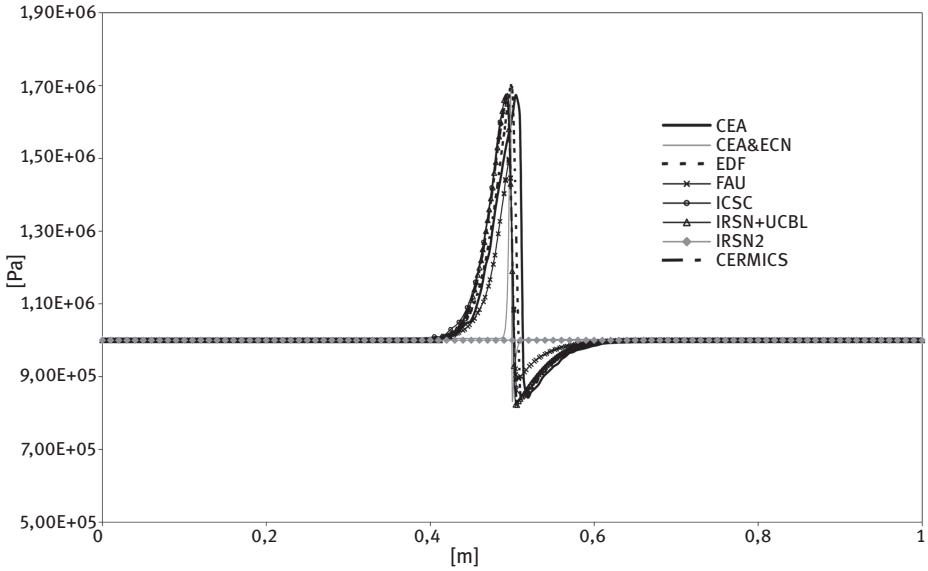

Figure 3.11: Test-case 2: Liquid pressure profiles, at $t = 10$ s.

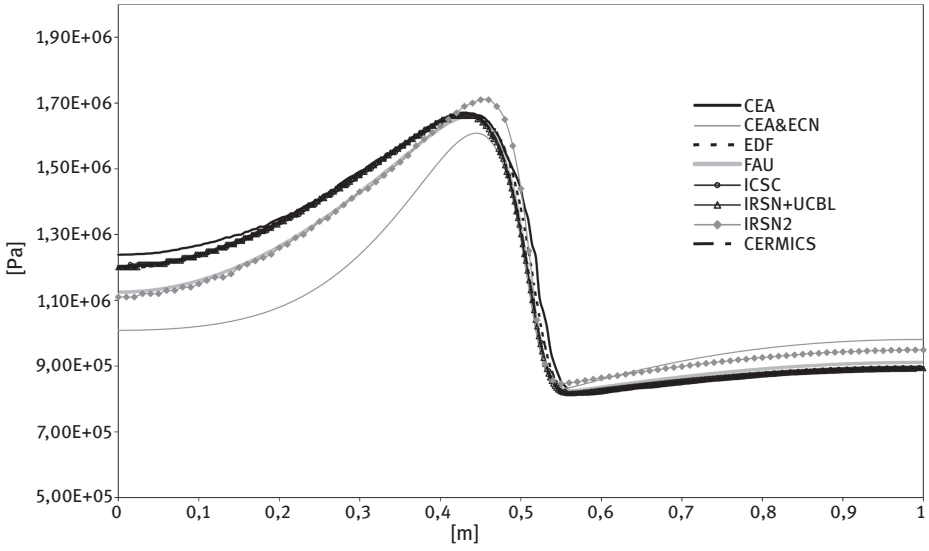

Figure 3.12: Test-case 2: Liquid pressure profiles, at $t = 1000$ s.

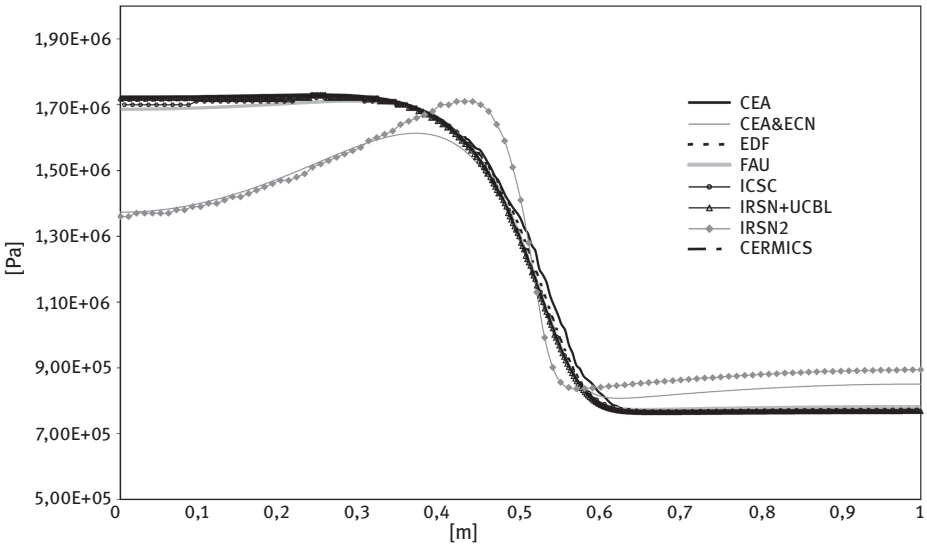

Figure 3.13: Test-case 2: Liquid pressure profiles, at $t = 5000$ s.

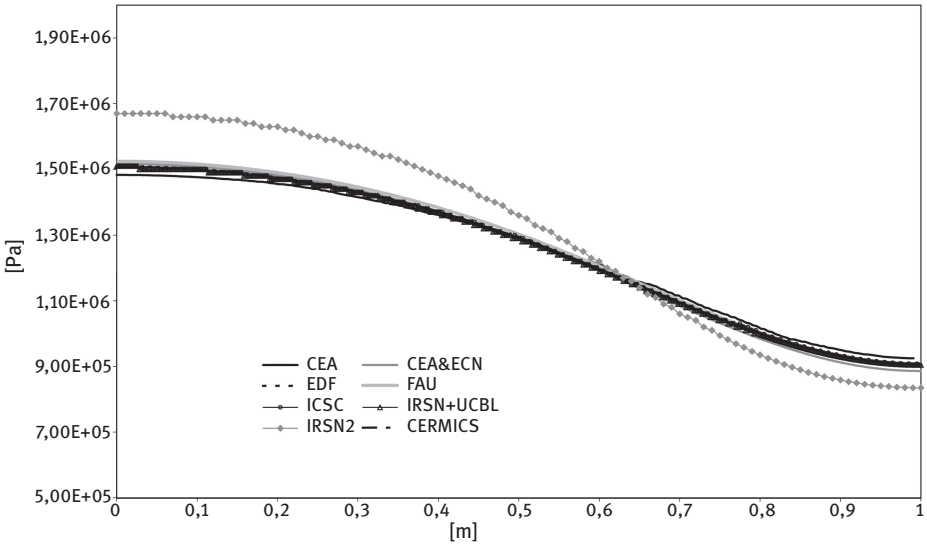

Figure 3.14: Test-case 2: Liquid pressure profiles, at $t = 50\,000$ s.

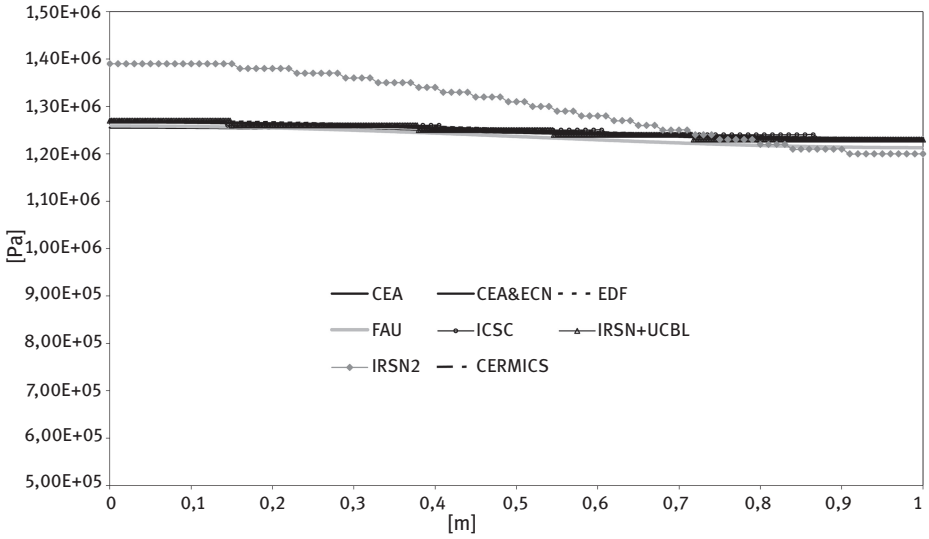

Figure 3.15: Test-case 2: Liquid pressure profiles, at $t = 1\,000\,000$ s

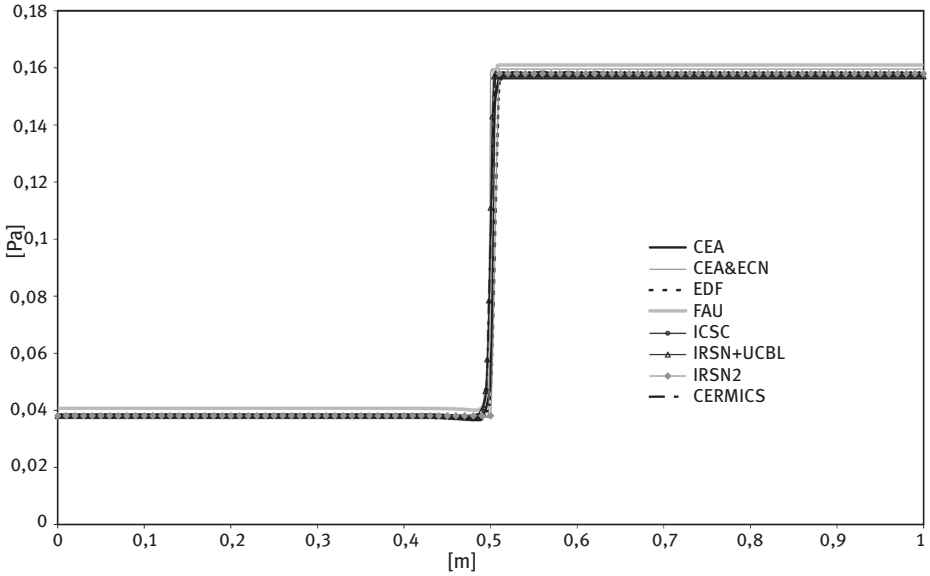

Figure 3.16: Test-case 2: Gas saturation profiles, at $t = 10$ s

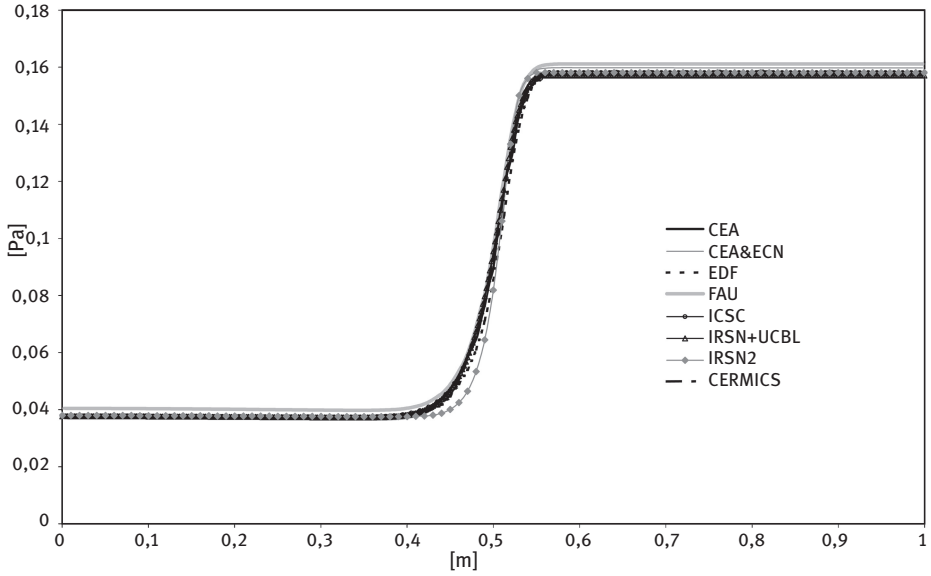

Figure 3.17: Test-case 2: Gas saturation profiles, at $t = 1000$ s

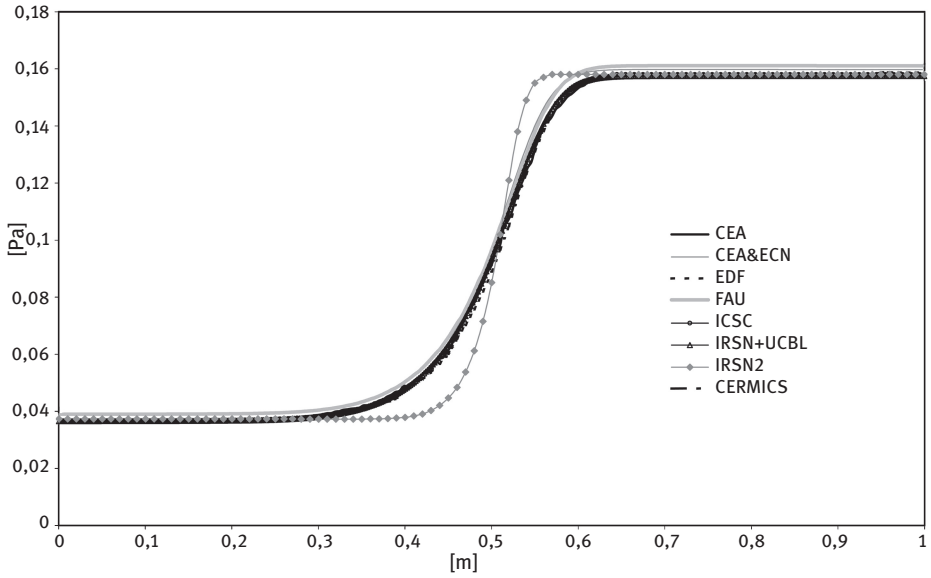

Figure 3.18: Test-case 2: Gas saturation profiles, at $t = 5000$ s

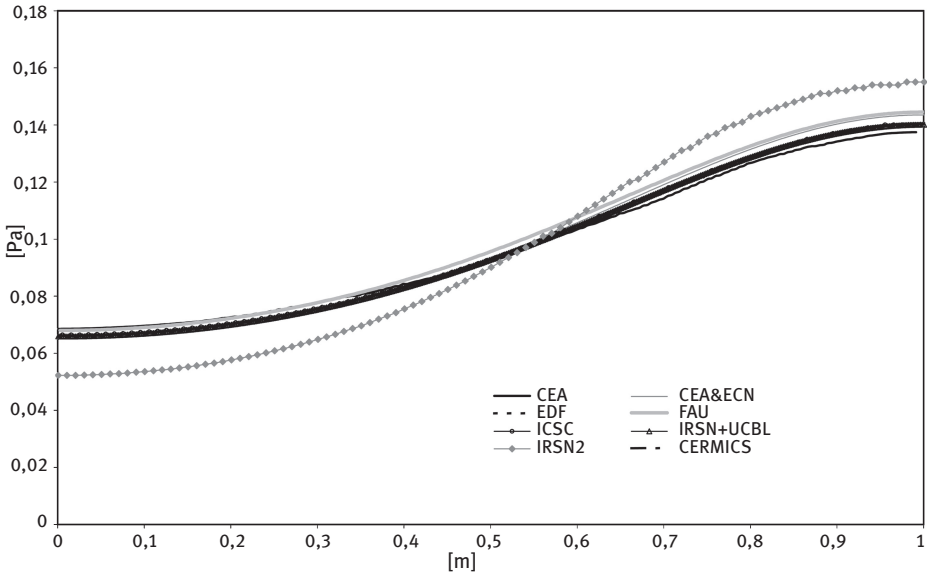

Figure 3.19: Test-case 2: gas saturation profiles, at $t = 50\,000$ s

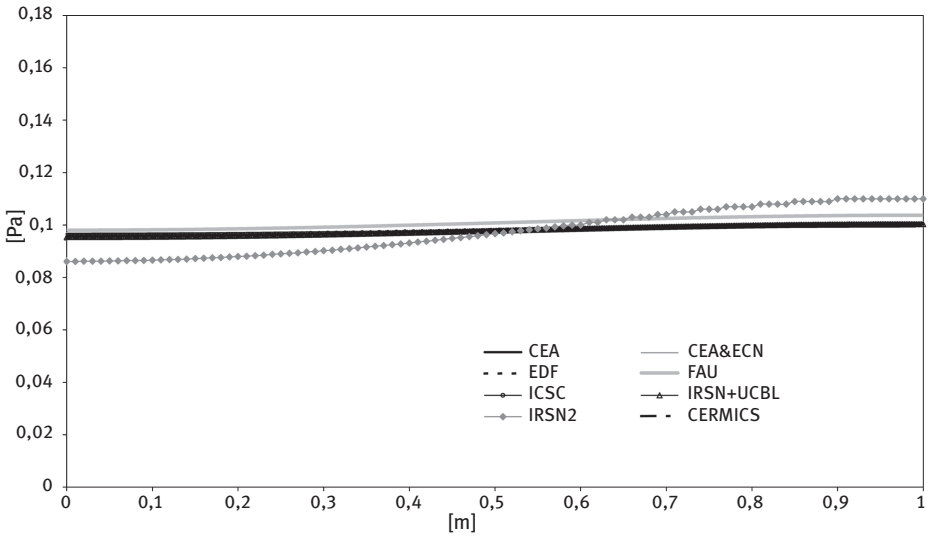

Figure 3.20: Test-case 2: Gas saturation profiles, at $1\,000\,000$ s

6 Conclusions and perspectives

These two test cases were part of a benchmark submitted to the scientific community [1–3]. All the exercises were based on a very simple domain geometry and used a standard physical model (isothermal and nonreactive flow) but they aim to highlight some of the very specific difficulties encountered in numerical simulation of gas migration in underground repositories.

In all the types of situations where physics is quite complex, there is no point in checking the pure numerical accuracy of a code as is not confident of the quality of the physical modeling on which this code is based. Before testing the numeric and algorithmic simulations it is necessary to be sure that the simulations are really simulating the real physical process. This is why the aim of these two tests was to focus on the model efficiency rather than on the numerical methods quality. Once this first step is completed, it will be possible to make assessment on pure numerical accuracy (solver strategies, computational cost, time stepping, and algorithm).

The first test case investigated the ability of numerical simulators to handle phase appearance and disappearance in two-phase compositional flow with interphase mass transfer. For this exercise, it is necessary to use a true miscible model and find the appropriate choice of primary variables. Finally, only six teams participated successfully. Most of the results are qualitatively similar, even if some differences remain (mainly in the amplitude of minima and maxima). Further investigation is needed to clearly understand the role played by the strategy's choice for solving the algebraic system and the solubility conditions.

The second test has consisted of simulating the evolution of a compressible two-phase flow, starting from an "out of equilibrium" initial state. The main and only focus of this test case was to study the relaxation of a nonequilibrium initial state and how the mechanical balance was restored. Accordingly, we studied a situation where a true miscible model was not really required; as a result, height teams were able to participate. As for the first exercise, outputs of all the teams show very similar phenomena and tendencies; all results remain rather close despite few differences, probably due to time discretization.

The main conclusions are then:

- according to the mathematical model they have chosen; not all the teams were able to do the tests;
- mainly only models using a set of persistent variables were able to pass the first test;
- once eliminated, the codes which were not using suitable mathematical model, and hence unable to compete; it appears that all the results show same tendencies and little differences and that the spatial scheme choice did not make any difference.
- the differences in results are probably due to either the strategy used for solving the algebraic system, including the solubility conditions, or the time step management.

While remaining in the same spirit, i.e. checking the interphase mass transfer model efficiency and robustness, the undergoing extensions of this benchmark will be done in two directions:

- to complete and extend this benchmark to strong gravity effects, pressure entrance jump (like in Brook Corey), 100 % desaturated media;
- to assess the pure numerical accuracy (solver strategies, computational cost, time stepping, and algorithm).

But, in order to broaden our scope (NAPL remediation, petroleum engineering, CSS), we would also be interested in a next step, to introduce more complex phenomenological aspects such as temperature variation, chemical reaction, or geochemical effects.

References

[1] Exercices de qualification numérique de codes; Numerical Test Data Base; http://sources.univ-lyon1.fr/cas_test.html

[2] Benchmarks; Benchmarks en cours, Écoulements diphasiques; http://www.gdrmomas.org/ex_qualifications.html

[3] S. Granet, Benchmark multiphasique. Journées Scientifiques du GNR MoMaS CIRM Marseille 2–4 novembre 2011; http://sources.univ-lyon1.fr/cas_test/MoMasBenchDiphasique_ppt.pdf

[4] Safety of Geological Disposal of High-level and Long-lived Radioactive Waste in France, OECD NEA No. 6178 (2006); http://www.oecd-nea.org/rwm/reports/2006/nea6178-argile.pdf

[5] A. Bourgeat, M. Jurak, and F. Smaï, Two-phase partially miscible flow and transport modeling in porous media: application to gas migration in a nuclear waste repository, *Comp. Geosciences.*, Volume 13 (2009), Number 1, 29–42.

[6] A. Bourgeat, M. Jurak, and F. Smaï, Modelling and Numerical Simulation of gas migration in a nuclear waste repository, (2010) arXiv:1006.2914v1 [math.AP].

[7] A. Bourgeat, M. Jurak, and F. Smaï, On persistent primary variables for numerical modeling of gas migration in a nuclear waste repository, *Comp. Geosciences.*, Volume 17 (2013), Number 2, 287–305, DOI 10.1007/s10596-012-9331-1

[8] A. Ern and I. Mozolevski, Discontinuous galerkin method for two-component liquid-gas porous media flows, *Comp. Geosciences.*, **16** (2012), 677–690.

[9] J. Talandier, Synthèse du benchmark couplex-gaz. *Journées scientifiques du GNR MoMaS, Lyon, 4–5 septembre 2008;* http://momas.univ-lyon1.fr/presentations/couplex_lyon2008_andra.ppt

[10] http://sources.univ-lyon1.fr/cas_test/Cas_test_couplex_gaz_1.pdf

[11] http://sources.univ-lyon1.fr/cas_test/Cas_test_couplex_gaz_2.pdf

[12] *FORGE project*; http://www.forgeproject.org

[13] Draft report on definition of benchmark studies on repository-scale numerical simulations of gas migration, *FORGE Reports*, D1.1; http://www.bgs.ac.uk/forge/docs/reports/D1.1.pdf, 2009.

[14] Progress report on benchmark studies on repository-scale numerical simulations of gas migration, *FORGE Work Packages 2 Reports*, D1.3; http://www.bgs.ac.uk/forge/docs/reports/D1.3.pdf, March 2010.

[15] K. Pruess, C. Oldenburg, and G. Moridis, *Tough2 User's Guide*, version 2.0., (1999) Lawrence Berkeley National Laboratory, Berkeley.

[16] B. Flemisch, M. Darcis, K. Erbertseder, B. Faigle, A. Lauser, K. Mosthaf, S. Müthing, P. Nuske, A. Tatomir, M. Wolff, and R. Helmig, DuMux: DUNE for Multi-Phase, Component, Scale, Physics. *Advances in Water Resources.* **34(9)** (2011), 1102–1112.

[17] H. Class, R. Helmig, and P. Bastian, Numerical simulation of non-isothermal multiphase multicomponent processes in porous media 1. An efficient solution technique, *Adv. Water Resour.* **25** (2002), 533–550.

[18] P. A. Forsyth, A. J. A. Unger, and E. A. Sudicky, Nonlinear iteration methods for nonequilibrium multiphase subsurface flow, *Adv. Water Resour.* **21** (1998), 433–449.

[19] Panday, S., P. A. Forsyth, R. W. Falta, Yu-Shu Wu, and P. S. Huyakorn: Considerations for robust compositional simulations of subsurface nonaqueous phase liquid contamination and remediation, *Water Resour. Res.* **31** (1995), 1273–1289.

[20] Y.-S. Wu and P. A. Forsyth: On the selection of primary variables in numerical formulation for modeling multiphase flow in porous media, *J. Cont. Hydr.* **48** (2001), 277–304.

[21] S. Kräutle, The semismooth Newton method for multicomponent reactive transport with a minerales, *Adv. Water Res.* **34** (2011), 137–151.

[22] F. Facchinei and J. S. Pang, *Finite Dimensional Variational Inequalities and Complementarity Problems*, Springer, New York (2003).

[23] S. Bütikofer and D. Klatte: A nonsmooth Newton method with path search and its use in solving $C * 1, 1$ programs and semi-infinite problems,*SIAMJO* **20**, No. 5 (2010), 2381–2412.

[24] J. Jaffré and A. Sboui, Henry's Law and Gas Phase Disappearance, *Transp. Porous Media.* **82** (2010), 521–526.

[25] I. Ben Gharbia and J. Jaffré, Gas phase appearance and disappearance as a problem with complementarity constraints *Mathematics & Computers in Simulation*, accepted (To appear), 2013.

[26] A. Lauser, C. Hager, R. Helmig, and B. Wohlmuth, A new approach for phase transitions in miscible multi-phase flow in porous media. *Water Resour.* **34** (2011), 957–966.

[27] K. Ito and K. Kunish, On a semi-smooth Newton method and its globalization, *Math. Program. Ser. A* **118** (2009), 347–370.

[28] M. Hintermuller, K. Ito, and K. Kunisch, The primal-dual active set strategy as a semi-smooth Newton method, *SIAM J. Optim.* **13** (2002), 865–888.

[29] O. Angelini, C. Chavant, E. Chénier, R. Eymard, and S. Granet, Finite VolumeApproximation of a diffusion-dissolution model and application to nuclear waste storage. *Mathematics & Computers in simulation.* **81** (2011), 2001–2017.

[30] R. Neumann, P. Bastian, and O. Ippisch, Modeling Two-Phase Two-Component Flow with Disappearing Gas Phase, *Comp. Geosciences.* Volume 17 (2012), Number 1, 139–149, DOI 10.1007/s10596-012-9321-3.

[31] P. Bastian, M. Blatt, A. Dedner, C. Engwer, J. Fahlke, C. Gärser, R. Klofkörn, M. Nolte, M. Ohlberger, and O. Sander, DUNE, Distributed and Unified Numerics Environment (2011); http://www.dune-project.org

[32] http://www.code-aster.org

[33] F. Caro, B. Saad, and M. Saad, Two-Component Two-Compressible Flow in a Porous Medium, *Acta Appl. Math.* **117** (2012), 15–46.

[34] B. Saad, Modélisation et simulation numérique d'écoulement multi-composants en milieux poreux, *Phd Thesis, Ecole Centrale Nantes* (2011).

[35] E. Marchand, T. Müller, and P. Knabner, Fully Coupled Generalised Hybrid-Mixed Finite Element Approximation of Two-Phases Two-Component Flow in Porous Media. Part II: Numerical Scheme and Numerical Results, *Comp. Geosciences.* **16**, Number 3 (2012), 691–708.

[36] E. Marchand, T. Müller, and P. Knabner, Fully Coupled Generalised Hybrid-Mixed Finite Element Approximation of Two-Phases Two-Component Flow in Porous Media. Part I: Formulation and Properties of the Mathematical Model, *Comp. Geosciences.* Volume 17 (2013), Number 2, 431–442.

[37] Journée Modèlisation des écoulements diphasiques liquide-gaz en milieu poreux: cas tests et résultats, MoMaS – Paris, 23 septembre 2010; http://momas.univ-lyon1.fr/journees_cas_tests_momas_23-09-10.html